

Silicon Organic Hybrid Technology—A Platform for Practical Nonlinear Optics

Prototype devices have demonstrated that efficient optical modulators made up of layers of silicon and organic material can be constructed at moderate cost.

By JUERG LEUTHOLD, *Senior Member IEEE*, WOLFGANG FREUDE, *Senior Member IEEE*, JAN-MICHAEL BROSI, ROEL BAETS, *Fellow IEEE*, PIETER DUMON, IVAN BIAGGIO, MICHELLE L. SCIMECA, FRANÇOIS DIEDERICH, BRIAN FRANK, AND CHRISTIAN KOOS

ABSTRACT | A cost-effective route to build electrically as well as optically controlled modulators in silicon photonics is reviewed. The technology enables modulation at bit rates beyond 100 Gbit/s. This platform relies on the well-established silicon-based complementary metal-oxide-semiconductor processing technology for fabricating silicon-on-insulator (SOI) waveguides, while an organic cladding layer adds the required nonlinearity. The strength of this hybrid technology is discussed, and two key devices in communications are exemplarily regarded in more detail. The first device demonstrates demultiplexing of a 120 Gbit/s signal by means of four-wave mixing in a slot-waveguide that has been filled with a highly nonlinear $\chi^{(3)}$ -organic material. The second device is a 100 Gbit/s/1 V electrooptic modulator based on a slow-light

SOI photonic crystal covered with a $\chi^{(2)}$ -nonlinear organic material.

KEYWORDS | Nonlinear optics; phase modulators; silicon-on-insulator technology

I. INTRODUCTION

Silicon photonics is likely to become a key technology for highly integrated optics, such as it has been for electronics for more than 60 years. The main advantages of silicon as a platform for integrated optics are the availability of a mature silicon technology, the compatibility with complementary metal-oxide-semiconductor (CMOS) electronics, low costs, and the availability of a high-resolution lithography with 35 nm resolution [1]–[5]. Consequently, a whole industry has worked on providing a complete library of optical components. Some of these components are lowest loss waveguides [6], [7], tapers [8] and grating couplers [9], filters [10], [11], or photonic crystal devices offering dispersion and slow light functionalities [12], [13], to name just a few. While all of the aforementioned devices are passive building blocks, active devices such as lasers, amplifiers, and modulators are needed to complement the library of multifunctional optoelectronic silicon circuits. And indeed, by wafer-bonding III–V heterostructures onto silicon-on-insulator (SOI) waveguides, continuous-wave (cw) lasers [14]–[16], mode-locked lasers [17], and optically and electrically pumped amplifiers [18]–[20] have been realized. Yet, electrical and optical modulation is still an issue. As a matter of fact, electrical and optical signal processing suffer from

Manuscript received November 5, 2008; revised January 29, 2009. Current version published June 12, 2009. This work was supported in part by Deutsche Forschungsgemeinschaft (DFG), DFG Center for Functional Nanostructures, in the Priority Program SP 1113 “Photonic Crystals,” by the Initiative of Excellence, University of Karlsruhe, by the European project EURO-FOS, and by Deutsche Telekom Stiftung. The work of I. Biaggio and B. Frank was supported in part by the Commonwealth of Pennsylvania, Ben Franklin Technology Development Authority. The work of F. Diederich and B. Frank was supported by the ETH Research Council. **J. Leuthold**, **W. Freude**, and **J.-M. Brosi** are with the Institute of Photonics and Quantum Electronics, University of Karlsruhe, 76131 Karlsruhe, Germany (e-mail: leuthold@etit.uka.de; W.freude@ihq.uni-karlsruhe.de; Brosi@ipq.uni-karlsruhe.de). **R. Baets** and **P. Dumon** are with the Photonics Research Group, Ghent University-IMEC, B-9000 Gent, Belgium (e-mail: roel.baets@ugent.be; pdumon@intec.ugent.be). **I. Biaggio** and **M. L. Scimeca** are with the Department of Physics, Lehigh University, Bethlehem, PA 18015 USA (e-mail: biaggio@Lehigh.EDU; Scimeca@Lehigh.EDU). **F. Diederich** and **B. Frank** are with the Laboratorium für Organische Chemie, Swiss Federal Institute of Technology, CH-8093 Zürich, Switzerland (e-mail: diederich@org.chem.ethz.ch; Frank@org.chem.ethz.ch). **C. Koos** was with the Institute of Photonics and Quantum Electronics, University of Karlsruhe, 76131 Karlsruhe, Germany. He is now with Carl Zeiss AG, Corporate Research and Technology, 73447 Oberkochen, Germany (e-mail: c.koos@zeiss.de).

Digital Object Identifier: 10.1109/JPROC.2009.2016849

two-photon absorption (TPA) and free-carrier absorption (FCA) related speed limitations [21].

While research in silicon concentrates on solving these speed issues, polymer optics have achieved remarkable results long since. Already in 1997, nonlinear polymer devices demonstrated modulation over the whole W-band up to 110 GHz [22], and thus indicated the potential of organic materials for even highest speed. This has triggered the development of a big set of novel nonlinear organic materials [23].

A logical next step in the development was thus to combine the silicon and organic technologies in order to create a new silicon-organic hybrid (SOH) platform that combines the advantages of silicon with the ultrafast performance of organic materials. Indeed, potential operation in excess of 1 THz can be inferred [24], and only recently, high-quality 120 Gbit/s signal processing was performed [25], [26]. In addition, ultralow power electrooptic switching has been shown as well [27].

In this paper, we review the SOH platform. It relies on CMOS technology for fabricating silicon wire waveguides and exploits nonlinear organic materials for the cladding. While the silicon wire provides the guiding of the optical mode, the organic material provides the necessary nonlinearity to perform electrical and optical modulation up to highest speed. We first discuss approaches with structures for performing Kerr-based ultrafast $\chi^{(3)}$ -nonlinear signal processing and show that it is feasible to fabricate a slot waveguide structure, which provides a nonlinearity parameter on the order of $\gamma = 100\,000\text{ W}^{-1}\text{ km}^{-1}$. This is—to the best of our knowledge—the largest nonlinearity ever shown for a Kerr-effect based waveguide. We then demonstrate experimentally the demultiplexing of optical data signals from 120 to 10 Gbit/s in one compact device of 6 mm length [25]. Lastly, we give design guidelines that will lead the technology towards 100 Gbit/s/1 V modulators with dimensions of $80\ \mu\text{m}$ [28].

This paper is organized as follows. In Section II, we outline two major applications areas, the state-of-the-art, and issues with current approaches. In Section III, we discuss structures and design principles for waveguides that will enable all-optical signal processing at bit rates beyond 100 Gbit/s. Section IV gives design guidelines for next-generation electrooptical SOH modulators. This paper ends with conclusions.

II. ULTRAFAST OPTICAL AND ELECTRICAL PROCESSING: APPLICATIONS AND ISSUES WITH CURRENT TECHNOLOGY

The ability to electrically process optical signals is key for the fabrication of high-speed optoelectronic modulators. Modulators are needed for the fabrication of small form factor transceivers, which preferentially should comprise all the electrical and optical circuitry on a single low-cost

silicon chip. Fig. 1 shows the outline of such a chip with an integrated transmitter and receiver module. The chip could potentially be smaller than $2 \times 10\text{ mm}^2$. It could comprise a III–V wafer-bonded laser diode, a high-speed electro-optic modulator to encode data onto an optical carrier provided by the laser diode, passive optical waveguides, a silicon-germanium photodiode, and CMOS compatible electronic circuitry. However, electrical modulation of optical signals in silicon is not straightforward because the second-order $\chi^{(2)}$ -susceptibility is non-existent in principle in monocrystalline silicon, and thus simple electrooptic modulation of the optical phase is not possible. As a consequence, injection of free carriers can be used instead. These carrier-injection operated modulators have already shown operation up to 40 Gbit/s [29]. However, free carriers lead to increased losses, and it is not clear to what extent speed can be further increased due to the limited mobility and the relatively long carrier lifetime.

The situation is similar for all-optical signal processing in silicon. To optically modulate optical signals, a sufficiently strong third-order $\chi^{(3)}$ -susceptibility is needed. While third-order nonlinearities in silicon nanophotonic waveguides exist, the effect is impeded by TPA and by TPA-induced FCA. For instance, all-optical signal regeneration has been demonstrated at 10 Gbit/s [30], but for data rates of 40 Gbit/s, free carriers generated by TPA have to be removed by appropriate technological measures for preventing excessive absorption [29], [31], and this becomes actually difficult at bit rates beyond 40 Gbit/s. While all-optical technologies are already of interest at both lower and highest speeds due to the small footprint and the resulting energy efficiency, they are, however,

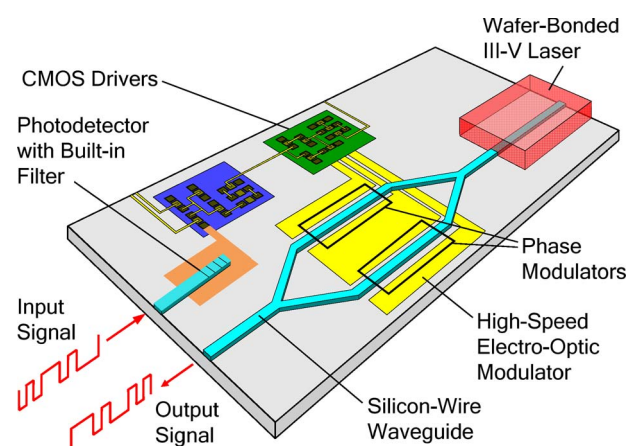


Fig. 1. Schematic view of a silicon transceiver chip, comprising a III–V wafer-bonded cw laser source, a high-speed electrooptic amplitude modulator with its electronic CMOS driving circuitry, and the receiver part made of a monolithically integrated photodiode with built-in filter. The amplitude modulator is realized by inserting two phase modulator sections in both arms of a Mach-Zehnder interferometer.

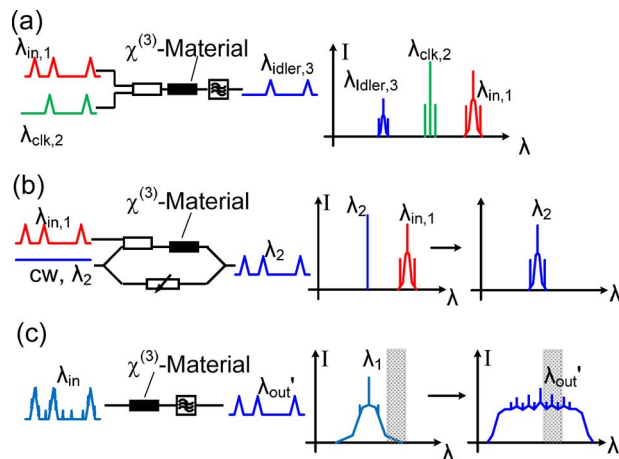


Fig. 2. High-speed all-optical signal processing enabled by $\chi^{(3)}$ -nonlinear materials. (a) Demultiplexing by four-wave mixing. (b) All-optical wavelength conversion by cross-phase modulation in an interferometric configuration. (c) All-optical signal regeneration by self-phase modulation.

most attractive at speeds beyond the present limits of electronics, i.e., at speeds beyond 40 Gbit/s.

At those speeds, $\chi^{(3)}$ -nonlinearities allow manifold applications. For instance, four-wave mixing (FWM) [30] is frequently used for all-optical high-speed demultiplexing [25], for wavelength conversion, or for optical sampling. Fig. 2(a) shows a typical FWM setup, in which a high-speed data signal at $\lambda_{in,1}$ is demultiplexed by a strong clock signal $\lambda_{clk,2}$, resulting in an idler signal at $\lambda_{idler,3}$. In this example, the clock signal maps every second bit of the input signal onto an idler by means of the $\chi^{(3)}$ -nonlinearity. The spectrum behind the $\chi^{(3)}$ -nonlinear device is depicted on the right-hand side of Fig. 2(a). A filter is typically used to separate the new signal at $\lambda_{idler,3}$ from the input and the clock signal.

For other applications, cross-phase modulation (XPM) might be used to perform wavelength conversion; see Fig. 2(b). In this process, a strong input signal $\lambda_{in,1}$ changes the refractive index of the $\chi^{(3)}$ -nonlinear material. This affects the phase of a second signal, e.g., a cw signal at λ_2 . This can actually be exploited in an interferometric configuration by transfer of the original information at $\lambda_{in,1}$ onto a new wavelength at λ_2 . XPM nonlinearity is attractive because it allows wavelength conversion over the largest possible spectral range since the phase-matching condition is always fulfilled.

Finally, self-phase modulation (SPM) may be used to perform all-optical signal regeneration; see Fig. 2(c). SPM-based signal regeneration usually follows the so-called Mamyshev scheme [32], in which the intensity-induced refractive index change is exploited to spectrally broaden a signal. A subsequent filter selects only those parts of the spectrum that were caused by moderate signal powers. The noisy low-power contributions will not have sufficient power to broaden the signal and thus will not make it into the filter

passband. Conversely, signals with large amplitude will experience stronger broadening and thus generate spectral components beyond the filter passband. These additional spectral components will be rejected. As a result, both the noisy low-power parts of the signal and the high-power parts will be suppressed, thus regenerating the signal.

III. SILICON ORGANIC HYBRID PLATFORM

The motivation behind the SOH approach is to combine the advantages of silicon technology with the versatility offered by the numerous options with organic materials.

In the SOH approach, all passive components, i.e., waveguides, couplers, and filters, are fabricated in silicon. The high refractive index of silicon ($n \approx 3.5$) leads to strongly guided light. The nonlinear optical functionality, however, is taken over by the organic cladding. For choosing this material, one takes advantage of the many organic molecules and polymers that have been developed in the last years. Their nonlinear refractive index virtually reacts instantaneously, and so the bandwidth is almost unlimited [24]. Organic materials typically have small linear refractive indexes on the order of 1.4–2.5.

Examples of electrooptically active nonlinear organic molecules and polymers and their electrooptic coefficients r are summarized in Table 1. Electrooptic coefficient r and second-order susceptibility $\chi^{(2)}$ are interrelated by

$$r = -2\chi^{(2)}/n_0^4. \quad (1)$$

Table 1 shows that many organic materials have electrooptic coefficients that significantly exceed the value specified for LiNbO₃.

Similarly, one has the choice between numerous nonlinear organic materials with favorable $\chi^{(3)}$ -susceptibilities. Table 2 lists the nonlinear index coefficient n_2 for various materials. Nonlinear index coefficient n_2 and susceptibility $\chi^{(3)}$ are interrelated by

$$n_2 = 3\text{Re}(\chi^{(3)})/(4\varepsilon_0 cn^2) \quad (2)$$

where ε_0 and c are dielectric constant and velocity of light in vacuum, respectively, and n is the linear refractive index of the nonlinear material. From Table 2, it is seen that

Table 1 Electrooptic Coefficients for Various $\chi^{(2)}$ -Nonlinear Materials

Material	λ [nm]	EO coefficient	Ref.
DSTMS	1555	$r_{11} = 25$ pm/V	[33]
AJ-CKL1	1310	$r_{33} = 133$ pm/V	[34]
Doped, crosslinked polymer	1550	$r_{33} = 170$ pm/V	[35]
LiNbO ₃	1500	$r_{33} \approx r_{42} = 30$ pm/V	

Table 2 Nonlinear Index Coefficient n_2 and TPA Figure of Merit (FOM) for Various $\chi^{(3)}$ -Nonlinear Materials

Material	λ [nm]	n	n_2 [m ² /W]	FOM	Ref.
Silicon	1500	3.48	6×10^{-18}	0,86	[36]
Silica	1550	1.45	$2,5 \times 10^{-20}$	10	[37]
Bismite glass	1550	2.02	$3,2 \times 10^{-19}$		[38]
Chalcogenide glass As ₄₀ Se ₆₀	1500	2,81	$2,3 \times 10^{-17}$	11	[39]
PDA	1319	1.5	4.8×10^{-18}	1.5	[40]
DDMEBT	1500	1.8	$2,0 \times 10^{-17}$	> 5	[41]

some chalcogenide glasses as well as some organic molecules like DDMEBT¹ [41] have a particularly large nonlinear index coefficient.

However, the suitability of a nonlinear material depends not only on the nonlinear index coefficient n_2 but also on the nonlinear losses. Most often, it is TPA that leads to strong absorption. Unfortunately, the TPA-generated carriers occupy excited band states. These carriers with lifetimes in the nanosecond range then act as highly absorptive plasma that reduces the optical power and thereby degrades the nonlinear performance. A frequently used figure of merit (FOM), which relates the nonlinear phase shift to the associated intensity change, is defined by

$$\text{FOM} = \frac{1}{\lambda} \frac{n_2}{\alpha_2} \quad (3)$$

where α_2 is the nonlinear absorption coefficient. Table 2 shows that silicon—although having a relatively large n_2 -coefficient—is unfortunately burdened with a low TPA FOM. Conversely, silica has a large FOM yet weak nonlinear characteristics. On the other hand, chalcogenide glasses or the organic molecule DDMEBT show both a large nonlinear coefficient n_2 and a small nonlinear absorption coefficient α_2 , thus leading to a good FOM.

In waveguides, it is not just the material dependent refractive index but also the confinement of the mode that needs optimization in order to achieve the maximum nonlinearity. The nonlinearity parameter γ is

$$\gamma = \frac{2\pi}{\lambda} \frac{n_2}{A_{\text{eff}}^{(3)}} \quad (4)$$

It depends significantly on the effective area $A_{\text{eff}}^{(3)}$ for third-order nonlinear interaction [42].

We will discuss below how one could take advantage of the waveguide geometry and the refractive index for maximizing γ . This will lead us to a design with a nonlinearity parameter, which we believe to be the highest one ever demonstrated for a Kerr medium.

¹2-[4-(dimethylamino)phenyl]-3-[[4-(dimethylamino)phenyl]ethynyl]buta-1,3-diene-1,1,4,4-tetracarbonitrile.

IV. HIGH-SPEED ALL-OPTICAL NONLINEAR DEVICES

In this section, we discuss the potential of the SOH platform for the fabrication of a device performing all-optically $\chi^{(3)}$ -nonlinear operations at speeds beyond 100 Gbit/s. Our design goal is the fabrication of a nonlinear waveguide with a nonlinearity parameter γ beyond 100 000 W⁻¹ km⁻¹. This value is five orders of magnitude larger than the nonlinearity parameter γ in a silica fiber. Key to the success is the possibility to:

- optimize the geometry of the waveguide independently of the nonlinear material;
- take advantage of the electric field enhancement across materials with different refractive indexes;
- select an organic material with the highest possible nonlinear susceptibility combined with a low TPA coefficient.

We will end the section with a demonstration of an all-optical 120 to 10 Gbit/s demultiplexing experiment.

A. Optimization of SOH Platform for Record Nonlinearity?

1) *SOH Waveguide for Nonlinear Operation:* The stronger the confinement of the optical field in the nonlinear material is (the smaller $A_{\text{eff}}^{(3)}$ is), the larger the nonlinearity parameter γ becomes. Here we discuss three structures optimized for the strongest quasi-TE mode confinement (dominant electric field component E_x oriented along the substrate plane): the strip waveguide with core nonlinearity, the strip waveguide with cover nonlinearity, and the slot waveguide with cover nonlinearity; see Fig. 3. Similar results can actually be found for quasi-TM modes (dominant electric field component E_y oriented perpendicularly to the substrate plane) [42].

We first discuss the optimum geometry of a strip waveguide with a nonlinear core. Fig. 3(a) shows the electric field magnitude of the fundamental quasi-TE mode. If only the waveguide core provides the nonlinearity, it is advantageous to choose a nonlinear material with the highest possible linear refractive index. Silicon with a refractive index of $n = 3.48$ is a good choice [30]; alternatively, chalcogenide glass has shown good results as well [43]. The width w and the height h of the waveguide core then need to be optimized for the smallest possible effective area $A_{\text{eff}}^{(3)}$.

The right-hand side of Fig. 3(a) shows the minimum $A_{\text{eff}}^{(3)}$ that can be obtained if the optimum width and height is chosen and for a cladding refractive index n_{cover} that varies between 1.0 and 2.5. For silicon, $A_{\text{eff}}^{(3)} = 0.1 \mu\text{m}^2$ can be achieved for a cladding refractive index of $n_{\text{cover}} = 1.8$, a core width $w = 400$ nm, and a core height $h = 220$ nm [42].

A strip waveguide with cladding nonlinearity is depicted in Fig. 3(b). If the nonlinearity is dominated by the cover material, then the waveguide dimensions must

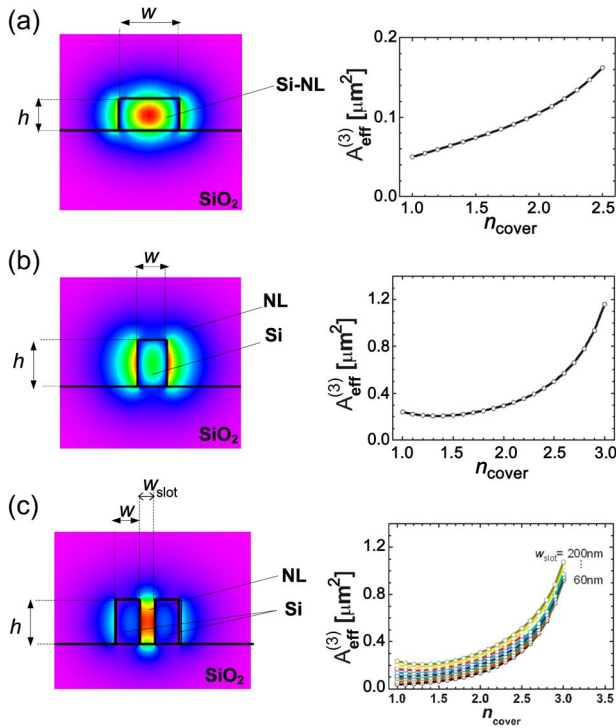


Fig. 3. Magnitude of quasi-TE electric field (dominant electric field component oriented horizontally, along the substrate plane). Minimum effective areas $A_{\text{eff}}^{(3)}$ for a cover material with a linear refractive index n_{cover} . The structures are optimized for maximum (a) core nonlinearity in a strip waveguide, (b) cover nonlinearity in a strip waveguide, and (c) cover nonlinearity in a slot waveguide.

be tuned such that a large portion of the field is pushed into the cladding. An $A_{\text{eff}}^{(3)}$ of $0.2 \mu\text{m}^2$ can be achieved for a cladding refractive index of $n_{\text{cover}} = 1.8$, a core width $w = 220 \text{ nm}$, and a core height $h = 400 \text{ nm}$ [42].

Finally, if the silicon slot waveguide structure of Fig. 3(c) is chosen, an $A_{\text{eff}}^{(3)}$ smaller than $0.1 \mu\text{m}^2$ can be obtained for a slot width of 60 nm , a core width $w = 180 \text{ nm}$, and a core height $h = 350 \text{ nm}$ [42]. The unique advantage of the slot waveguide structure is that it concentrates the field inside the slot, so that the nonlinearities in the silicon material become unimportant, and the slot material dominates the nonlinear behavior. The slot can be filled with a nonlinear organic substance, which can be chosen from a large number of species. In fact, nonlinear organic materials with low refractive indexes and nonlinearities that excel the ones provided by silicon are available; see Table 2.

2) *Electric Field Enhancement in the Cladding:* An inherent advantage of structures with the nonlinearity in the cover material is the possibility to enhance the electromagnetic field at the interface of the high-index core to the low-index cladding. Actually, the electric field normal to the interface results from the required

continuity of the normal component D_x of the dielectric displacement

$$D_{x,\text{Si}} = D_{x,\text{slot}} \rightarrow \epsilon_{\text{Si}} E_{x,\text{Si}} = \epsilon_{\text{slot}} E_{x,\text{slot}}. \quad (5)$$

For instance, if $n_{\text{slot}} = 1.8$ and $n_{\text{Si}} = 3.5$, the enhancement of the electric field in the slot over the electric field in the silicon amounts to a factor of $\epsilon_{\text{Si}}/\epsilon_{\text{slot}} = (n_{\text{Si}}/n_{\text{slot}})^2 = 3.8$. This is illustrated in Fig. 4.

The enhancement of the normal electric field in the organic cover material over the field in the waveguide is relevant for two reasons:

- TPA and free carriers generated by TPA are ultimately limiting the speed in silicon devices. It is therefore important to keep signal intensities in silicon low, while they should be high in the nonlinear material. For the slot waveguide approach, TPA in silicon scales with the intensity as

$$\text{TPA}_{\text{Si}} \sim \alpha_{\text{TPA,Si}} I_{\text{Si}}^2 \sim \alpha_{\text{TPA,Si}} I_{\text{slot}}^2 \left(\frac{\epsilon_{\text{slot}}}{\epsilon_{\text{Si}}} \right)^4. \quad (6)$$

This actually means that even though the intensity I_{slot} in the slot is high, chances for TPA in silicon are 200 times smaller than if the field was concentrated in silicon; this factor holds true for our case where $n_{\text{slot}} = 1.8$ and $n_{\text{Si}} = 3.5$.

- $\chi^{(3)}$ -nonlinearities scale with the square of the dominant field, i.e., in all cases where one exploits (partially) degenerate FWM, XPM, or SPM, one benefits from the square law of the field enhancement. In our example with $n_{\text{slot}} = 1.8$ and $n_{\text{Si}} = 3.5$, we would benefit from a nonlinearity enhancement by as much as 14.

3) *Nonlinear Organic Material:* Large nonlinearities are typically achieved by compounds that have large

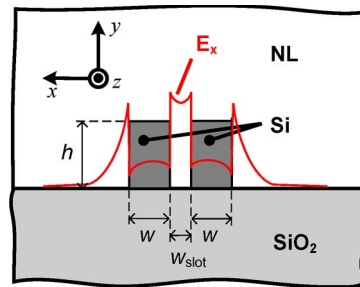


Fig. 4. Cross-section of slot waveguide with two silicon (Si) ribs on a silicon dioxide buffer layer (SiO2) covered by a nonlinear material (NL). For a quasi-TE mode, the magnitude of the dominant electric field component E_x is enhanced inside the slot.

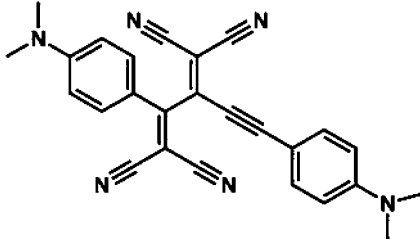


Fig. 5. Molecular structure of the organic molecule DDMEBT.

delocalized electron systems. Carbon atoms offer a multitude of compounds with such delocalized electron systems, and they show extraordinarily large optical nonlinearities that allow highest speed modulation [23].

The substance DDMEBT is a small organic molecule with a linear refractive index $n = 1.8 \pm 0.1$ and a nonlinear index coefficient $n_2 \approx (1.7 \pm 0.8) \times 10^{-17} \text{ m}^2/\text{W}$, Fig. 5. It has large isotropic, off-resonant third-order susceptibility $\chi^{(3)} \approx (2 \pm 1) \times 10^{-19} \text{ m}^2/\text{V}^2$ at a wavelength of $1.5 \mu\text{m}$. The molecular substance is effectively transparent for wavelengths beyond 700 nm . Since this corresponds to a bandgap that is twice as large as the energy of the operating wavelength, a low TPA coefficient is to be expected.

B. Fabrication of SOH Slot Waveguide

Slot waveguide templates have been fabricated on a 200 mm CMOS pilot line using 193 nm deep ultraviolet lithography on an ASML PAS5500/1100 stepper and a chlorine-based reactive ion etching process [44]. The thickness of the device layer (waveguide height) amounts to $h = 220 \text{ nm}$, and the buried oxide is $2 \mu\text{m}$ thick. The strip (slot) widths w (w_{slot}) range from 160 to 220 nm (150 to 250 nm). A scanning electron microscope (SEM) picture of the slot waveguide is shown in Fig. 6.

The waveguide templates were functionalized by vapor deposition of a 950-nm -thick amorphous organic film consisting of DDMEBT [41]. The compound is described in more detail as derivative 2 in [45]. After deposition, cross-sectional profiles of the waveguides have been produced by focused ion beam milling using a Carl Zeiss CrossBeam

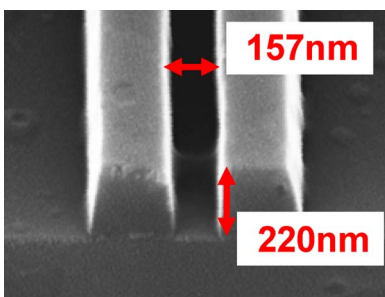


Fig. 6. SEM picture of slot waveguide structure.

system. The silicon waveguide strips exhibit a slightly trapezoidal shape. Yet, a high homogeneity of the organic cover layer over its whole cross-section was found, and it could be confirmed that the organic substance homogeneously fills the slot without forming any voids. This is a key feature of the material and its deposition process that enables the effective realization of the SOH concept.

C. Experimental Characterization

1) *Loss*: For high index-contrast waveguides, roughness of the core-cladding interface leads to scattering loss and is regarded the main contributor to overall losses [46]. A cutback method was applied to obtain the linear propagation power loss coefficient α , together with the fiber-chip coupling loss α_{cp} . We found propagation losses of $\alpha = 1.5 \text{ dB/mm}$ and $\alpha_{\text{cp}} = 6 \text{ dB}$ within the spectral range from 1500 to 1575 nm . The waveguide dimension of the characterized structure was $h = 220 \text{ nm}$, the top width of the trapezoidal silicon strips was $w = 216 \text{ nm}$, and the corresponding slot width was $w_{\text{slot}} = 157 \text{ nm}$ [25].

2) *The Nonlinearity Parameter*: The silicon organic hybrid slot waveguide provided nonlinearity parameters γ up to $116\,000 \text{ W}^{-1} \text{ km}^{-1}$. This is, to the best of our knowledge, the largest Kerr nonlinearity measured so far in a waveguide structure.

The nonlinearity parameter γ of the waveguide was obtained by measuring the conversion efficiency η of partially degenerate FWM, applying a cw pump and a cw signal. For a waveguide of geometrical length L and nonlinearity parameter γ , the conversion efficiency is given by

$$\eta = \exp(-\alpha L) (\gamma P_p L_{\text{eff}})^2. \quad (7)$$

P_p denotes the on-chip pump power just after the input facet of the waveguide. The effective waveguide length $L_{\text{eff}} < L$ accounts for both linear propagation loss and group-velocity dispersion and is given by [26]

$$L_{\text{eff}} = \frac{\sqrt{1 + \exp(-2\alpha L) - 2 \exp(-\alpha L) \cos(\Delta\beta L)}}{\sqrt{\alpha^2 + \Delta\beta^2}}$$

$$\Delta\beta = \frac{\pi c D_2 \Delta\lambda^2}{2\lambda_p^2}, \quad \Delta\lambda = |\lambda_s - \lambda_c|$$

$$2\lambda_p^{-1} = \lambda_s^{-1} + \lambda_c^{-1}. \quad (8)$$

The quantity $\Delta\beta$ represents the phase mismatch due to group velocity dispersion (GVD) between the signal wave at wavelength λ_s and the converted wave at wavelength λ_c . The quantity D_2 denotes the GVD parameter and λ_p is the wavelength of the pump.

Measuring two different samples with nominally identical geometry at two different signal wavelengths, we have

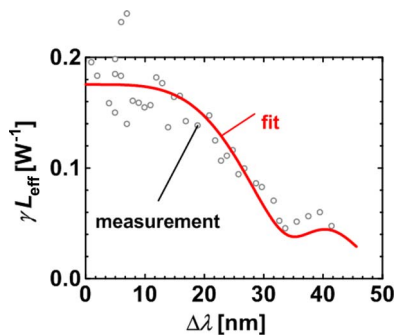


Fig. 7. Dependence of FWM conversion efficiency on detuning $\Delta\lambda$; measurement (\circ) and fit ($-$). The launched on-chip pump power after the input facet of the waveguide was $P_p = 11.0$ dBm.

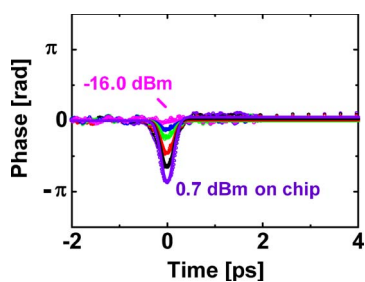


Fig. 8. Pump-probe experiment showing ultrafast phase response of a SOH slot waveguide. No slow tail from TPA with its associated free-carrier absorption is observed.

obtained nonlinear parameters γ of 116 000, 107 000, 104 000, and 91 000 $\text{W}^{-1} \text{km}^{-1}$, leading to an average value of 104 000 $\text{W}^{-1} \text{km}^{-1}$ [25].

3) *Phase-Matching Over Large Spectral Range:* The dependence of the FWM efficiency as a function of wavelength offset between pump and probe signal has been tested as well; see Fig. 7. The group velocity dispersion parameter D_2 was found to be so small that phase-matching over a large 20 nm spectral range could be achieved. Measurements of the spectral efficiency were performed on a waveguide with height $h = 220$ nm, width $w = 216$ nm, slot width $w_{\text{slot}} = 157$ nm, and geometrical waveguide length $L = 4$ mm. By fitting the measured dependence of η as a function of the detuning $\Delta\lambda$ to (7) and (8), the waveguide under test exhibited a group velocity dispersion parameter of $D_2 = -6.84$ fs/(mm nm) and a nonlinearity parameter of $\gamma = 0.83 \times 10^5 \text{ W}^{-1} \text{ km}^{-1}$.

4) *Dynamics and Two-Photon Absorption:* The SOH slot waveguide was tested for its phase response in a pump-probe experiment [47]. Fig. 8 shows the phase shift induced by a pump-probe measurement with 100 fs long pulses for various input powers at a wavelength of 1550 nm. The slot waveguide shows an instantaneous Kerr-type response, which has its origin predominantly in the cladding. There are no slow tails due to TPA in silicon with subsequent free-carrier absorption such as seen in nonlinear silicon strip waveguides [47]. The geometry of the slot waveguides in the TPA absorption experiment was identical to the one from the loss characterization.

D. All-Optical 120 to 10 Gbit/s Demultiplexing

To prove the viability of the concept, all-optical demultiplexing of a 120 Gbit/s data signal to a 10 Gbit/s data stream has been performed. The experimental setup together with the eye diagrams are depicted in Fig. 9. For the data (pump), we used mode-locked fibre lasers operating at repetition rates of 10 GHz and emitting pulses of approxi-

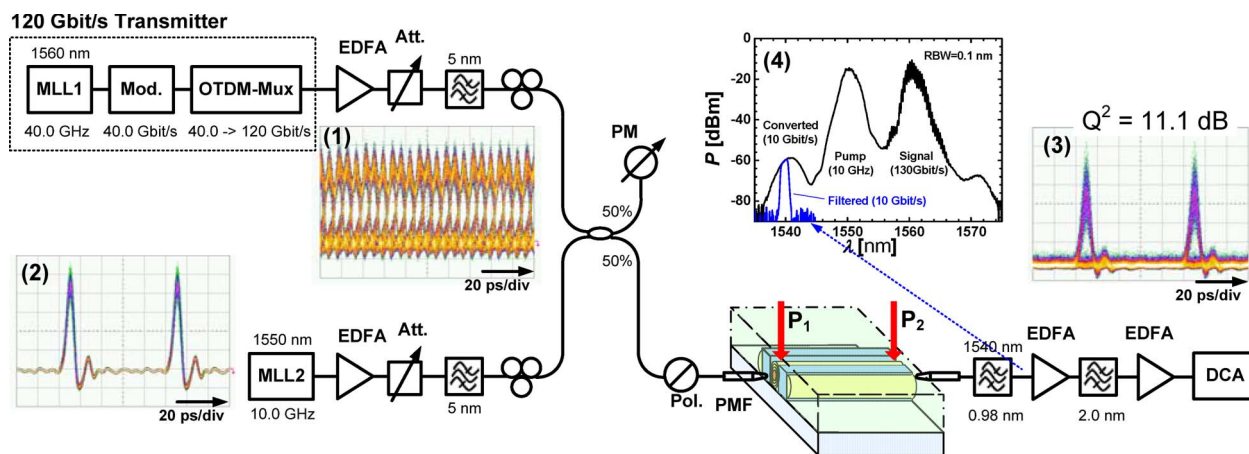


Fig. 9. Experimental setup of the demultiplexing experiment; MLL1, MLL2: mode-locked lasers; Mod: data modulator; OTDM-Mux: optical time-division multiplexer; EDFA: erbium-doped fiber amplifier; Att: attenuator; BP: optical bandpass; PM: power meter; Pol: polarizer; PMF: polarization maintaining fiber; DUT: device under test; DCA: digital communication analyzer. Inset: spectrum at the output of the DUT (black) and after bandpass filtering (blue).

mately 3 ps full-width half-maximum. The signal and the pump were synchronized using a tunable optical delay. The 120 Gbit/s data were generated by modulating the 10 GHz pulse train with a pseudorandom bit sequence ($2^{31}-1$ bit) and by subsequent optical time-division multiplexing. Both the pump and the signal were amplified and coupled into a SOH slot waveguide of height $h = 220$ nm, strip width $w = 212$ nm, and slot width $w_{\text{slot}} = 205$ nm. The output signal was bandpass filtered at the converted wavelength and amplified, and the eye diagram was recorded with a digital communication analyzer. By varying the delay between the pump and the signal, different tributaries could be chosen for demultiplexing. Similar performance was found for all the tributaries. From the eye diagram, a quality factor of $Q^2 = 11.1$ dB was measured for an on-chip pump power of 15.6 dBm (36 mW). Since the power of the converted signal depends quadratically on the pump power, and since the 10 GHz pump exhibits noticeable amplitude fluctuations [see eye diagram (2) in Fig. 9], the Q-factor was mainly limited by the performance of the pump.

More recently we have tested slot waveguides for their ability to demultiplex 170.8 to 42.7 Gbit/s [26] and for 40 Gbit/s all-optical wavelength conversion [48]. No pattern dependence or any other speed limitations were observed.

V. HIGH-SPEED SILICON-ORGANIC MODULATORS

In this section, we discuss the potential of the SOH platform for the fabrication of optical modulators with drive voltages around 1 V and bandwidths exceeding 100 Gbit/s [28].

Electrooptic modulators typically are implemented as Mach-Zehnder interferometers (MZIs); see Fig. 1, where both arms of the MZI comprise phase modulator sections.

Three phase modulator structures compatible with the SOH approach are depicted in Fig. 10. The phase shifters consist of silicon waveguides (Si) surrounded by a poled electrooptic organic material (EO). The optical strip waveguides are operated in quasi-TE mode. In the traveling-wave strip waveguide scheme of Fig. 10(a), the microwave field is applied via two aluminum conductors running in parallel to the optical strip waveguide. The spacing between the conductors and the optical waveguide is chosen large enough (typically $1 \mu\text{m}$) to avoid optical loss. For the traveling-wave socket slot waveguide [Fig. 10(b)], both silicon strips are doped and connected to the aluminum conductors by thin silicon sockets. Arsenic doping with a density of $n_D \approx 2 \times 10^{16} \text{ cm}^{-3}$ yields sufficient electrical conductivity $\sigma_{\text{Si}} \approx 10 (\Omega\text{cm})^{-1}$ but does not induce relevant optical loss. In Fig. 10(c), a photonic crystal (PhC) line defect waveguide comes with a slot etched into the SOI device layer for exploiting the field enhancement in quasi-TE polarization as described previously. The PhC is a slow-light structure, which significantly increases the interaction time with the

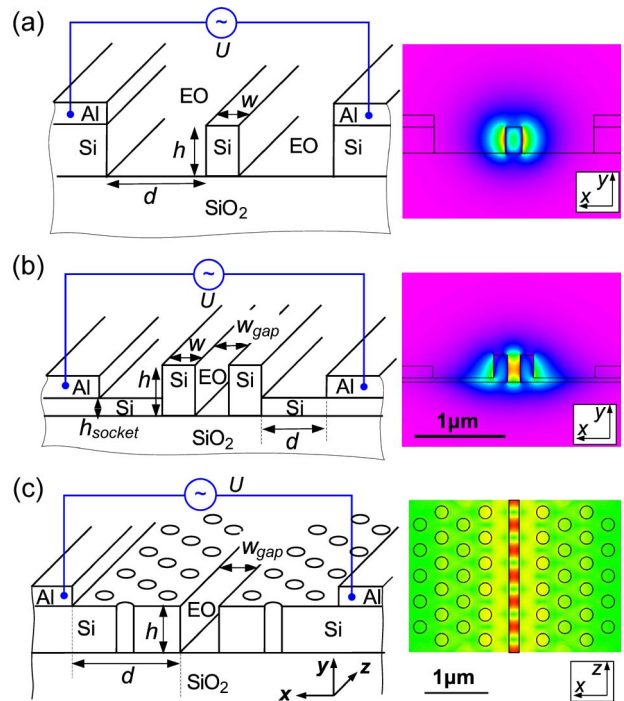


Fig. 10. Three implementations of silicon organic hybrid electrooptic modulators comprising silicon ribs on top of the buried oxide (SiO_2) and an electrooptic cover. The electric field magnitudes are depicted on the right-hand side. (a) Traveling-wave strip waveguide structure; (b) traveling wave slot waveguide structure; and (c) photonic crystal slot waveguide structure.

microwave field. This in turn allows the construction of ultracompact modulators. The numerous possibilities to arrange the PhC holes allow optimization of the structure so that operation without dispersion is possible within a sufficiently large wavelength range. Details of the PhC design, which resulted in light propagating at 4% of the speed of light in vacuum, have been published in [28] and [50] and demonstrated in [51]–[54]. The slot PhC modulator is covered with an EO material too. Again, the doped PhC regions are electrically connected to the aluminum conductors. The rationale for the slot waveguide modulator approach is as follows.

- The SOH allows filling of the slot with a highly nonlinear poled electrooptic material of choice, providing almost instantaneous nonlinearity—rather than direct carrier injection in silicon with its related speed limitations.
- The voltage applied across the electrodes drops off almost entirely across the narrow slot w_{gap} . Since the dimension of the slot is as small as 150 nm, one obtains a large electric field E_x right in the middle of the slot.
- The slot waveguide structure leads to an optical field almost entirely confined to the slot. This results in an extremely efficient optoelectronic

effect since now both the electric and optical field are largest inside the slot.

- The slow-light slot waveguide PhC approach provides an additional field enhancement of the optical field. This enhancement is due to the long time that the optical field resides in the structure and allows one to further reduce the length of the phase modulator section.

In the following, we will discuss important parameters such as modulation bandwidth f_{mod} and drive voltage swing, which are related to the π phase shift voltage U_π .

A. Modulation Bandwidth

In this section, we estimate the achievable modulation bandwidth under the assumption that the microwave generator is matched to the wave impedance of the coplanar transmission line of the MZI modulator, see Fig. 1. We further make the realistic assumption that the silicon structures are so small that microwave losses are negligible. The modulation bandwidth is then affected by RC effects, the spatial walkoff between the electrical and optical wave, and potential bandwidth limitations from the nonlinear material. However, the latter is negligible as long as there is no TPA and operation speed is not in the terahertz regime.

1) *Electrical RC-Limitations:* Electrical RC-limitations are negligible for an impedance-matched travelling-wave electrical waveguide as depicted in Fig. 10(a), yet there might be a limiting RC-factor for the two slot waveguide structures of Fig. 10(b) and (c). The doped sections connecting the metal electrodes and the slot have a finite resistivity R' per length, and the voltage across the nonconductive slot has a certain capacitance C' per length. As a result, an electrical wave with a constant amplitude U traveling along the electrodes generates a voltage amplitude U_{gap} across the nonconductive gap. The 3 dB bandwidth associated with the phase-shifter section as depicted in Fig. 11 is therefore [28].

$$f_{\text{RC},3\text{ dB}} = \frac{1}{4\pi R' C'} \quad (9)$$

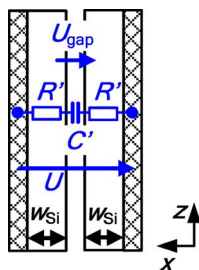


Fig. 11. Lumped-element model of the slot-structure.

Table 3 Dimensions of Strip, Slot, and Slot Photonic Crystal Phase Modulator Structures

Structure	w [nm]	w_{gap} [nm]	h [nm]	h_{socket} [nm]	d [μm]	L [mm]
Strip	260	N.A.	220	N.A.	1.0	5.1
Slot	235	150	220	70	1.0	1.3
Slot PhC	N.A.	150	220	N.A.	3.0	0.08

where $C' = \epsilon_0 n_{\text{cover}}^2 h / w_{\text{gap}}$ and $R'^{-1} = \sigma F h_{\text{slab}} / w_{\text{Si}}$ with w_{Si} being the width of the doped silicon section between aluminum electrode and slot.

2) *Walkoff Limitations:* The bandwidth limitation due to the walkoff between the optical field and the electromagnetic forward-travelling wave (negative sign) or a potentially reflected wave (positive sign) can be approximated reasonably well by [28], [55]

$$f_{\text{walkoff},3\text{ dB}} \cong \frac{0.5}{|t_{g,\text{opt}} \mp t_{g,\text{el}}|} = \frac{0.5}{L} \frac{1}{|1/v_{g,\text{opt}} \mp 1/v_{g,\text{el}}|} \quad (10)$$

where $v_{g,\text{opt}}$ and $v_{g,\text{el}}$ are the group velocities of the optical and the electrical waves and $t_{g,\text{opt}}$ and $t_{g,\text{el}}$ are the respective group delays of the waves propagating along the phase-shifter section. For the slow-light PhC structure, $t_{g,\text{opt}} \gg t_{g,\text{el}}$ holds, and no electrical traveling-wave structure with termination resistance is needed. An intuitive derivation for this relation has been given in [28].

3) *Quantitative Comparison of the SOH Modulators:* To quantitatively estimate the achievable bandwidth, we performed calculations using the parameters in Table 3. The lengths of the modulators were chosen such that a full modulation is obtained with a small voltage swing U of 1 V. This corresponds to a 2 V peak-to-peak voltage, which provides a phase shift of $\pi/2$ in each of the MZI arms. Since this phase shift is applied to each of the two MZI arms, a full π phase shift can be obtained if operating in push-pull mode. For the calculations, we have further assumed a conductivity of $\sigma = 10 \Omega^{-1} \text{ cm}^{-1}$ in the conductive silicon parts ($n_{\text{D}} \approx 2 \times 10^{16} \text{ cm}^{-3}$) and a filling factor F of 0.67 for the PhC slot waveguide.

The modulation bandwidths for the modulators depicted in Fig. 10 are listed in Table 4. The calculation shows that both the travelling wave and the photonic crystal slow-light structure provide modulation bandwidths in the 100 GHz range. The good performance is due to the fact that the electric field is largest in the slot—this is exactly where the optical field is almost entirely confined. The bandwidth limitation of the strip waveguide is due to the walkoff between electric and optical wave. It could be

Table 4 Achievable Modulation Bandwidths for Modulators in Fig. 10

Structure	$v_{g,opt}/c$	f_{RC}	$f_{walk-off}$
Strip	31 %	—	31 GHz
Slot	33 %	136 GHz	196 GHz
Slot PhC	4 %	118 GHz	76 GHz

overcome at the expense of higher voltage swings. Table 4 also shows that the PhC approach has led to an eightfold slow-down of the group velocity of the optical signal. As a consequence, the slow-light phase shifters potentially can be as short as 80 μm .

Although the large modulation bandwidths in Table 4 have yet to be proven experimentally, they are indicative for the potential of the platform. Preliminary experiments show that the technology seems to be viable.

B. Drive Voltage

The SOH approach allows operation of modulators with exceptionally low voltage swings [13]. To get a deeper insight, it is necessary to derive an equation that relates the voltage needed to induce the π phase shift across a phase modulator with its geometry. In [28], such an expression was derived as

$$U_{\pi} = \frac{\lambda}{n_{\text{cover}}^3} \frac{w_{\text{Electr}}}{r_{33}} \frac{1}{L\Gamma}. \quad (11)$$

In (11), λ is the vacuum wavelength of the optical field, r_{33} the electrooptic coefficient, and n_{cover} the refractive index across the gap. For the calculations in Table 4, we have assumed $r_{33} = 80 \text{ pm/V}$ and $n_{\text{cover}} = 1.6$. The distance within which the electric modulation field drops is denoted as w_{Electr} . In the strip waveguide structure of Fig. 10(a), for example, it would actually be $w_{\text{Electr}} = 2d + w$, whereas in slot structures, the field drops within $w_{\text{Electr}} = w_{\text{gap}}$. The modulator length is L , and Γ is the field interaction factor. It quantifies the strength of the nonlinear EO interaction of modulating electric field and optical mode in a unit cell along a lattice period a

$$\Gamma = \frac{\int_{\text{EO region}} \frac{n}{Z_0} |\hat{E}_x|^2 dV}{\int_{\text{Unit cell}} \Re(\hat{E} \times \hat{H}^*) \cdot \mathbf{e}_z dV} \propto \frac{1}{v_{g,opt}} \quad (12)$$

REFERENCES

- [1] Y. A. Vlasov, "Silicon photonics for next generation computing systems," presented at the ECOC 2008, Sep. 2008, paper Tu.1A.1.
- [2] M. Lipson, "Silicon photonics: An exercise in self control," *Nature Photon.*, vol. 1, pp. 18–19, Jan. 2006.
- [3] B. G. Lee and K. Bergmann, "Silicon nano-photonics interconnection networks in multicore processor systems," presented at the OSA Annu. Meeting, Rochester, NY, Oct. 2008, paper FTuS1.
- [4] T. F. Krauss, D. Beggs, A. di Falco, T. White, L. O'Faolain, C. Monat, M. Lee, and B. Eggleton, "Slow light for switching and nonlinear effects in SOI," presented at the OSA Annu. Meeting, Rochester, NY, Oct. 2008, paper FTuU3.
- [5] D. Van Thourhout, J. Van Campenhout, P. Rojo-Romeo, P. Regreny, C. Seassal, P. Binetti, X. J. M. Leijtens, R. Nötzel,

where Z_0 is the free-space wave impedance, \hat{E} (x -component E_x) and \hat{H} are the optical-mode electric and magnetic fields, and \mathbf{e}_z is the unit vector in z -direction. In the case of the strip and slot waveguide, the volume integrals can be replaced by surface integrals in a cross-section. The field interaction factor is different from the confinement factor, which is usually between zero and one. In a slow-light structure, the field interaction factor Γ might be considerably larger than one. It actually is a measure of the energy stored in the transverse component of the propagating optical mode inside the phase modulator.

Equation (11) shows that the combination of a) a slot waveguide where the voltage drops over a narrow gap $w_{\text{Electr}} = w_{\text{gap}}$ with b) a potentially strong field interaction factor Γ (inversely proportional to the group velocity $v_{g,opt}$) and c) a free choice of an optimum nonlinear material indeed provides lowest possible voltage swings with ultrashort modulator lengths.

Lastly, it should be noted that an MZI modulator is typically operated in push–pull mode. This way, $U_{\pi}/4$ is sufficient to fully modulate the MZI, where U_{π} is the voltage that induces a π phase shift in the modulator. Also, the lengths given in Table 4 relate to voltage swings $U_{\pi}/4 = 1 \text{ V}$.

VI. CONCLUSION

We reviewed a recently introduced silicon-on-insulator technology within which all-optical and electrooptic interaction is performed in organic cover layers rather than in the silicon core of SOI waveguides. This silicon organic hybrid approach has provided highest nonlinearities beyond $\gamma = 100\,000 \text{ W}^{-1} \text{ km}^{-1}$. As a result, all-optical signal processing has been performed at speeds beyond 100 Gbit/s on a 6 mm silicon chip with less than 16 dBm pump power. Theoretical considerations further show that the same technology is capable of designing electrically controlled silicon MZI modulators to speeds beyond 100 Gbit/s, applying voltage swings of 1 V for device lengths between 1.2 mm and 80 μm —depending on whether a slot waveguide traveling-wave approach or a slow-light slot waveguide design is chosen. ■

Acknowledgment

The authors acknowledge technological support by the European Network of Excellence ePIXnet (silicon photonics platform) and by ASML Netherlands B.V.; and an equipment loan from Siemens Portugal and from the Optoelectronics Research Centre, Southampton, U.K.

- M. K. Smit, L. Di Cioccio, C. Lagahe, J.-M. Fedeli, and R. Baets, "A photonic interconnect layer on CMOS," presented at the European Conf. Opt. Commun. (ECOC'07), Sep. 2007, paper 6.3.1.
- [6] T. Tsuchizawa, T. Watanabe, K. Yamada, T. Shoji, J. Takahashi, and S. Itabashi, "Microphotonics devices based on silicon microfabrication technology," *IEEE J. Sel. Topics Quantum Electron.*, vol. 11, pp. 232–240, Jan./Feb. 2005.
- [7] M. Lipson, "Guiding, modulating, and emitting light on silicon-challenges and opportunities," *J. Lightw. Technol.*, vol. 23, pp. 4222–4238, Dec. 2005.
- [8] R. Sun, M. Beals, A. Pomerene, J. Cheng, C. Hong, L. Kimmerling, and J. Michel, "Impedance matching vertical optical waveguide couplers for dense high index contrast circuits," *Opt. Express*, vol. 16, no. 16, p. 11682 ff., Jul. 2008.
- [9] T. Fukazawa, F. Ohno, and T. Baba, "Very compact arrayed-waveguide-grating demultiplexer using Si photonic wire waveguides," *Jpn. J. Appl. Phys.*, vol. 43, pp. L673–L675, Apr. 2004.
- [10] M. A. Popovic, T. Barwicz, M. S. Dahlem, F. Gan, C. W. Holzwarth, P. T. Rakich, M. R. Watts, H. I. Smith, F. X. Kärtner, and E. P. Ippen, "Hitless-reconfigurable and bandwidth-scalable silicon photonic circuits for telecom and interconnect applications," presented at the OSA Optical Fiber Commun. Conf. (OFC'08), May 2008, paper OTuF4.
- [11] W. Bogaerts, P. Taillaert, J. Wouters, S. Beckx, V. Wiaux, and R. Baets, "Compact wavelength-selective functions in silicon-on-insulator photonic wires," *IEEE J. Sel. Topics Quantum Electron.*, vol. 12, pp. 1394–1401, Nov. 2006.
- [12] Y. A. Vlasov, M. O'Bolye, H. F. Hamann, and S. J. McNab, "Active control of slow light on a chip with photonic crystal waveguides," *Nature*, vol. 438, pp. 65–69, Nov. 2005.
- [13] T. Baba, "Slow light in photonic crystals," *Nature Photon.*, vol. 2, p. 465 ff., Aug. 2008.
- [14] A. W. Fang, H. Park, O. Cohen, R. Jones, and M. J. Paniccia, "Electrically pumped hybrid AlGaInAs-silicon evanescent laser," *Opt. Express*, vol. 14, pp. 9203–9210, Sep. 2006.
- [15] H. Chang, A. W. Fang, M. N. Sysak, H. Park, R. Jones, O. Cohen, O. Raday, M. J. Paniccia, and J. E. Bowers, "1310 nm silicon evanescent laser," *Opt. Express*, vol. 15, pp. 11 466–11 471, Sep. 2007.
- [16] D. VanThourhout, J. Van Campenhout, R. Baets, P. Rojo-Romeo, P. Regreny, C. Seassal, P. Binetti, X. Leijtens, R. Ntzel, M. K. Smit, C. Lagahe, and J.-M. Fedeli, "A Photonic interconnect layer on CMOS," presented at the Eur. Conf. Opt. Commun. (ECOC'07), Sep. 2007, paper 6.3.1.
- [17] B. R. Koch, A. W. Fang, O. Cohen, and J. E. Bowers, "Mode-locked silicon evanescent lasers," *Opt. Express*, vol. 15, pp. 11 225–11 233, Aug. 2007.
- [18] R. L. Espinola, J. I. Dadap, R. M. Osgood, Jr., S. J. McNab, and Y. A. Vlasov, "Raman amplification in ultrasmall silicon-on-insulator wire waveguides," *Opt. Express*, vol. 12, pp. 3713–3718, Aug. 2004.
- [19] B. Jalali, O. Boyraz, D. Dimitropoulos, and V. Raghunathan, "Silicon Raman amplifier, laser, and their applications," presented at the SPIE Opt. East, Oct. 2005, paper #6014-2.
- [20] H. Park, A. W. Fang, R. Jones, O. Cohen, O. Raday, M. N. Sysak, M. J. Paniccia, and J. E. Bower, "A hybrid AlGaInAs-silicon evanescent amplifier," *IEEE Photon. Technol. Lett.*, vol. 19, pp. 230–232, May 2007.
- [21] Y. Liu and H. K. Tsang, "Time dependent density of free carriers generated by two photon absorption in silicon waveguides," *Appl. Phys. Lett.*, vol. 90, pp. 211–105, May 2007.
- [22] D. Chen, H. Fetterman, A. C. William, H. Steier, and L. R. Dalton, "Demonstration of 110 GHz electro-optic polymer modulation," *Appl. Phys. Lett.*, vol. 70, pp. 3335–3337, Apr. 1997.
- [23] J. M. Hales and J. W. Perry, *Introduction to Organic Electronic and Optoelectronic Materials and Devices*, S.-S. Sun and L. Dalton, Eds. Orlando, FL: CRC Press, May 2008, pp. 521–579.
- [24] M. Hochberg, T. Baehr-Jones, G. X. Wang, M. Shearn, K. Harvard, J. Liu, B. Chen, Z. Shi, R. Lawson, P. Sullivan, A. K. Y. Jen, L. Dalton, and A. Scherer, "Terahertz all-optical modulation in a silicon-polymer hybrid system," *Nature Mater.*, vol. 5, no. 9, pp. 703–709, Sep. 2006.
- [25] C. Koos, P. Vorreau, P. Dumon, R. Baets, B. Esembeson, I. Biaggio, T. Michinobu, F. Diederich, W. Freude, and J. Leuthold, "Highly-nonlinear silicon photonics slot waveguide," presented at the Conf. Opt. Fiber Commun. 2008 (OFC'2008), Feb. 2008, PDP25.
- [26] C. Koos, P. Vorreau, T. Vallaitis, P. Dumon, W. Bogaerts, R. Baets, B. Esembeson, I. Biaggio, T. Michinobu, F. Diederich, W. Freude, and J. Leuthold, "All-optical high-speed signal processing with silicon-organic hybrid slot waveguides," *Nature Photon.*, accepted for publication.
- [27] T. Baehr-Jones, B. Penkov, J. Huang, P. Sullivan, J. Davies, J. Takayasu, J. Luo, T.-D. Kim, L. Dalton, A. Jen, M. Hochberg, and A. Scherer, "Nonlinear polymer-clad silicon slot waveguide modulator with a half wave voltage of 0.25 V," *Appl. Phys. Lett.*, vol. 92, p. 163303, Apr. 2008.
- [28] J.-M. Brosi, C. Koos, L.-C. Andreani, M. Waldow, J. Leuthold, and W. Freude, "High-speed low-voltage electro-optic modulator with a polymer-infiltrated silicon photonic crystal waveguide," *Opt. Express*, vol. 16, pp. 4177–4191, Mar. 2008.
- [29] L. Liao, A. Liu, D. Rubin, J. Basak, Y. Chetrit, H. Nguyen, R. Cohen, N. Izhaky, and M. Paniccia, "40 Gbit/s silicon optical modulator for high-speed applications," *Electron. Lett.*, vol. 43, Aug. 2007.
- [30] R. Salem, M. A. Foster, A. C. Turner, D. F. Geraghty, M. Lipson, and A. L. Gaeta, "Signal regeneration using low-power four-wave mixing on silicon chip," *Nature Photon.*, vol. 2, pp. 35–38, 2008.
- [31] Y. Kuo, H. Rong, V. Sih, S. Xu, and M. Paniccia, "Demonstration of wavelength conversion at 40 Gb/s data rate in silicon waveguides," *Opt. Express*, vol. 14, pp. 11 721–11 726, Nov. 2006.
- [32] P. V. Mamyshev, "All-optical data regeneration based on self-phase modulation effect," in *Proc. Eur. Conf. Opt. Commun. (ECOC'98)*, Madrid, Spain, Sep. 1998, p. 475.
- [33] L. Mutter, F. D. Brunner, Z. Yang, M. Jazbinsek, and P. Günter, "Linear and nonlinear optical properties of the organic crystal DSTMS," *J. Opt. Soc. Amer. B*, vol. 24, pp. 2556–2561, Aug. 2007.
- [34] H. Chen, B. Chen, D. Hung, D. Jin, J. D. Luo, A. K.-Y. Jen, and R. Dinu, "Broadband electro-optic polymer modulators with high electro-optic activity and low poling induced optical loss," *Appl. Phys. Lett.*, vol. 93, p. 043507-2, Jul. 2008.
- [35] Y. Enami, C. T. Derose, D. Mathine, C. Loychik, C. Greenlee, R. A. Norwood, T. D. Kim, J. Luo, Y. Tian, A. K.-Y. Jen, and N. Peyghambarian, "Hybrid polymer/sol-gel waveguide modulators with exceptionally large electro-optic coefficients," *Nature Photon.*, vol. 1, pp. 180–185, May 2007.
- [36] H. K. Tsang, C. S. Wong, T. K. Liang, I. E. Day, S. W. Roberts, A. Harpin, J. Drake, and M. Asghari, "Optical dispersion, two-photon absorption and self-phase modulation in silicon waveguides at 1.5 μm wavelength," *Appl. Phys. Lett.*, vol. 80, pp. 416–418, Jan. 2002.
- [37] G. P. Agrawal, *Nonlinear Fiber Optics*, 3rd ed. San Diego, CA: Academic, 2001.
- [38] K. Kikuchi, K. Taira, and N. Sugimoto, "Highly nonlinear bismuth oxide-based glass fibers for all-optical signal processing," *Electron. Lett.*, vol. 38, p. 166, Feb. 2002.
- [39] J. M. Harbold, F. Ö. Ilday, F. W. Wise, J. S. Sanghera, V. Q. Nguyen, L. B. Shaw, and I. D. Aggarwal, "Highly nonlinear As-S-Se glasses for all-optical switching," *Opt. Lett.*, vol. 27, pp. 119–121, Jan. 2002.
- [40] P. D. Townsend, G. L. Baker, N. E. Schlotter, C. F. Klausner, and S. Eternad, "Waveguiding in spun films of soluble polydiacetylenes," *Appl. Phys. Lett.*, vol. 53, pp. 1782–1784, Nov. 1988.
- [41] B. Esembeson, M. L. Scimeca, I. Biaggio, T. Michinobu, and F. Diederich, "A high optical quality supramolecular assembly for third-order integrated nonlinear optics," *Adv. Mater.*, vol. 19, pp. 1–4, 2008.
- [42] C. Koos, L. Jacome, C. Poulton, J. Leuthold, and W. Freude, "Nonlinear silicon-on-insulator waveguides for all-optical signal processing," *Opt. Express*, vol. 15, no. 10, pp. 5976–5990, May 2007.
- [43] S. J. Madden, D.-Y. Choi, D. A. Bulla, A. V. Rode, B. Luther-Davies, V. G. Ta'eed, M. D. Pelusi, and B. J. Eggleton, "Long, low loss etched As₂S₃ chalcogenide waveguides for all-optical signal regeneration," *Optics Express*, p. 14414, Oct. 2007.
- [44] W. Bogaerts, P. Dumon, D. Van Thourhout, D. Taillaert, P. Jaenen, J. Wouters, S. Beckx, V. Wiaux, and R. G. Baets, "Compact wavelength-selective functions in silicon-on-insulator photonic wires," *IEEE J. Sel. Topics Quantum Electron.*, vol. 12, pp. 1394–1401, Nov./Dec. 2006.
- [45] T. Michinobu, J. C. May, J. H. Lim, C. Boudon, J.-P. Gisselbrecht, P. Seiler, M. Gross, I. Biaggio, and F. Diederich, "A new class of organic donor-acceptor molecules with large third-order optical nonlinearities," *Chem. Commun.*, pp. 737–739, Jan. 2005.
- [46] C. G. Poulton, C. Koos, M. Fujii, A. Pfrang, T. Schimmel, J. Leuthold, and W. Freude, "Radiation modes and roughness loss in high index-contrast waveguides," *IEEE J. Sel. Topics Quantum Electron.*, vol. 12, pp. 1306–1321, Nov./Dec. 2006.
- [47] T. Vallaitis, C. Koos, B. Esembeson, I. Biaggio, T. Michinobu, F. Diederich, P. Dumon, R. Baets, W. Freude, and J. Leuthold, "Highly nonlinear silicon photonics slot waveguides without free carrier absorption related speed-limitations," presented at the 34rd Eur. Conf. Opt. Commun. (ECOC'08), Brussels, Belgium, Sep. 2008, paper Th.2.D.6.
- [48] T. Vallaitis, C. Heine, R. Bonk, W. Freude, J. Leuthold, B. Esembeson, I. Biaggio, T. Michinobu, F. Diederich, P. Dumon, and R. Baets, "All-optical wavelength conversion at 42.7 Gbit/s in a 4 mm long silicon-organic

- hybrid waveguide,” presented at the Optical Fiber Commun. Conf. 2009 (OFC’2009), San Diego, CA, Mar. 2009, paper OWS3.
- [49] C. Koos, J.-M. Brosi, M. Waldow, W. Freude, and J. Leuthold, “Silicon-on-insulator modulators for next-generation 100 Gbit/s-Ethernet,” presented at the 33th Eur. Conf. Opt. Commun. (ECOC’07), Berlin, Germany, Sep. 2007, paper P056.
- [50] J.-M. Brosi, L. Leuthold, and W. Freude, “Microwave-frequency experiments validate optical simulation tools and demonstrate novel dispersion-tailored photonic crystal waveguides,” *J. Lightw. Technol.*, vol. 25, pp. 2502–2510, Sep. 2007.
- [51] L. H. Frandsen, A. V. Lavrinenko, J. Fage-Pedersen, and P. I. Borel, “Photonic crystal waveguides with semi-slow light and tailored dispersion properties,” *Opt. Express*, vol. 14, pp. 9444–9450, Oct. 2006.
- [52] J.-M. Brosi, C. Koos, L. C. Andreani, P. Dumon, R. Baets, J. Leuthold, and W. Freude, “100 Gbit/s/1 V optical modulator with slot slow-light polymer-infiltrated silicon photonic crystal,” in *OSA Topical Meeting Slow Fast Light (SL’08)*, Boston, MA, Jul. 13–16, 2008.
- [53] W. Freude, J.-M. Brosi, C. Koos, P. Vorreau, L. C. Andreani, P. Dumon, R. Baets, B. Esembeson, I. Biaggio, T. Michinobu, F. Diederich, and J. Leuthold, “Silicon-organic hybrid (SOH) devices for nonlinear optical signal processing,” presented at the 10th Int. Conf. Transparent Opt. Netw. (ICTON’08), Athens, Greece, Jun. 22–26, 2008, paper Tu.C2.1, vol. 2, pp. 84–87.
- [54] J. Li, T. P. White, L. O’Faolain, A. Gomez-Iglesias, and T. F. Krauss, “Systematic design of flat band slow light in photonic crystal waveguides,” *Optics Express*, p. 6227 ff., Apr. 2008.
- [55] S. Haxha, B. M. A. Rahman, and K. T. V. Grattan, “Bandwidth estimation for ultra-high-speed lithium niobate modulators,” *Appl. Opt.*, vol. 42, no. 15, p. 2674 ff., May 2003.

ABOUT THE AUTHORS

Juerg Leuthold (Senior Member, IEEE) received the master’s degree in physics (Dipl. Phys.) and the Ph.D. degree from the Swiss Federal Institute of Technology (ETH), Zürich, in 1991.

From 1992 to 1998, he was with the Micro- and Optoelectronics Institute, ETH. He has been involved in the modeling, design, and characterization of integrated all-optical devices for high-speed telecommunication applications. After a short postdoctoral period with Tokyo University, Tokyo, Japan, in spring 1999, he joined Bell Labs, Lucent Technologies, Holmdel, NJ, where he was affiliated from 1999 to June 2004. There he continued research on III-V semiconductors for high-speed telecommunication applications and performing system experiments with high-speed components. Since July 2004, he has been a Professor at the University of Karlsruhe, Germany, where he is Head of the Institute of Photonics and Quantum Electronics.

Dr. Leuthold is a Fellow of the Optical Society of America, a Senior Member of the IEEE Lasers and Electro-Optics Society, and a member of the German VDE. He has been a Program Chair of the Optical Amplifiers and Applications Meeting, a member of the Nonlinear Photonics meeting, and is currently a Committee Member of OFC, ECOC, and CLEO. He is the organizer of the OSA Optics and Photonics Congress 2010, Karlsruhe.



Jan-Michael Brosi received the M.Sc. degree from the Georgia Institute of Technology, Atlanta, in 2002 and the Dr.-Ing. (Ph.D.) degree from the University of Karlsruhe, Germany, in 2008.

He is currently working in the area of integrated silicon optics at the Institute of Photonics and Quantum Electronics, University of Karlsruhe, Germany. His research interests are design and characterization of photonic crystals and of fast electrooptic modulators.



Wolfgang Freude (Senior Member, IEEE) received the Dipl.-Ing. (M.S.E.E.) and Dr.-Ing. (Ph.D.E.E.) degrees in electrical engineering from the University of Karlsruhe, Germany, in 1969 and 1975, respectively.

He is a Professor at the Institute of Photonics and Quantum Electronics, University of Karlsruhe. His present research activities are in the design and fabrication of high-density integrated-optics devices and in photonic crystals. He has published more than 140 papers. He is a coauthor of *Optical Communications* (in German) (Berlin, Germany: Springer-Verlag, 1991). He authored or coauthored book chapters on “Multimode Fibres,” *Handbook of Optical Communications* (in German) (Berlin, Germany: Springer-Verlag, 2002) and “Microwave Modelling of Photonic Crystals,” *Photonic Crystals—Advances in Design, Fabrication, and Characterization* (Berlin, Germany: Wiley-VCH, 2004).

Prof. Freude is a member of Verband der Elektrotechnik Elektronik Informationstechnik Informationstechnische Gesellschaft (VDE/ITG), Germany, and OSA. He received an honorary doctoral degree from the Kharkov National University of Radioelectronics, Kharkov, Ukraine.



Roel Baets (Fellow, IEEE) received the bachelor’s degree from Ghent University, Belgium, in 1980 and the M.Sc. degree from Stanford University, Stanford, CA, in 1981, both in electrical engineering. He received the Ph.D. degree from Ghent University in 1984.

Since 1981, he has been with the Department of Information Technology (INTEC), Ghent University. Since 1989, he has been a Professor with the engineering faculty of Ghent University. From 1990 to 1994, he has also been a part-time Professor at the Technical University of Delft, The Netherlands. Since 2004, he also has been a part-time Professor at the Technical University of Eindhoven, The Netherlands. He has mainly worked in the field of photonic components. With about 250 journal publications and 500 conference papers as well as about 15 patents, he has made contributions to research on semiconductor laser diodes, passive guided wave and grating devices, and the design and fabrication of photonic ICs, both in III-V semiconductors and in silicon. He leads the Photonics Research Group at Ghent University-INTEC (associated lab of IMEC), which focuses on new concepts for photonic components and circuits for optical communication, optical interconnects, and optical sensing. He has been involved in various European research projects and has been Coordinator of some of them. Currently, he coordinates the European Network of Excellence ePIXnet.

Dr. Baets is a member of the Optical Society of America, IEEE Lasers and Electro-Optics Society (LEOS), SPIE, and Flemish Engineers Association. He has been member of the Program Committees of OFC, ECOC, the IEEE Semiconductor Laser Conference, ESSDERC, CLEO-Europe, LEOS Annual Meeting, Photonics Europe, and ECIO. He was Chairman of the IEEE-LEOS-Benelux chapter from 1999 to 2001. From 2003 to 2005, he was a member of the Board of Governors of IEEE-LEOS.



Pieter Dumon received the master's and doctoral degrees in electrical engineering from Ghent University, Belgium, in 2002 and 2007, respectively.

He is now at the Photonics group of IMEC-Ghent University, coordinating the ePIXfab initiative, which gives access to the CMOS facilities at IMEC (B) and CEA-LETI(F) for wafer-scale research and prototyping of silicon photonic components.

Dr. Dumon is a member of OSA.



François Diederich was born in Ettelbruck, Luxembourg, in 1952. He received the Dipl.-Chem. and Dr.rer.nat. degrees in chemistry from the University of Heidelberg, Germany, in 1977 and 1979, respectively, and the Habilitation degree from the Max-Planck-Institute for Medical Research, Heidelberg, Germany, in 1985.

From 1979 to 1981, he was a Postdoctoral Researcher with the University of California, Los Angeles (UCLA), in the Department of Chemistry and Biochemistry. He subsequently joined the Faculty of the Department of Chemistry and Biochemistry, UCLA, where he became a full Professor in 1989. In 1992, he became a Professor in the Department of Chemistry and Applied Biosciences, Swiss Federal Institute of Technology, Zürich. He works on molecular recognition and the preparation of carbon-rich advanced functional materials.



Ivan Biaggio received the master's (Dipl. Phys.) and Ph.D. degrees in physics from the Swiss Federal Institute of Technology (ETH), Zürich, in 1986 and 1993, respectively.

From 1993 to 1995, he was a Postdoctoral Researcher with the University of Southern California, Los Angeles, and the Institut d'Optique, Orsay, France. He then returned to ETH, where he obtained the *venia legendi* and was a Team Leader and "Privatdozent" until 2002, working on photo-refractive effects, nonlinear optics, and optoelectronics. In 2002, he joined Lehigh University, Bethlehem, PA, where he is now an Associate Professor of physics.



Brian Frank was born in Heidelberg, Germany, in 1978. He received the Dipl.-Chem. degree in chemistry from the Swiss Federal Institute of Technology, Zürich, in 2004, where he is currently pursuing the doctoral degree.

In 2005, he joined the group of Prof. F. Diederich in the Department of Chemistry and Applied Biosciences, ETH. He is working in the field of carbon-rich advanced functional materials with a strong focus on the design, synthesis, and characterization of new organic donor-acceptor chromophores as NLO materials.



Michelle L. Scimeca was born in 1983. She received the B.Sc. degree in physics and mathematics from Ramapo College of New Jersey, Mahwah, in 2006 and the M.S. degree in physics from Lehigh University, Bethlehem, PA, in 2008, where she is currently pursuing the Ph.D on topics in nonlinear optics.



Christian Koos was born in Heilbronn, Germany, in 1978. He received the Dipl.-Ing. (M.Tech.) and Dr.-Ing. (Ph.D.) degrees in electrical engineering from the University of Karlsruhe, Germany, in 2002 and 2007, respectively.

From 2007 to 2008, he was a Postdoctoral Researcher with the Institute of Photonics and Quantum Electronics, University of Karlsruhe. His research was focused on the modelling, fabrication, and characterization of integrated nanophotonic devices. He is now with the Corporate Research and Technology Department, Carl Zeiss AG, Oberkochen, Germany. He is working on nano-optical devices and on the optical characterization of nanostructured materials.

